VI. MICROWAVE ELECTRONICS*

Prof. L. D. Smullin	A. Bers	B. A. Highstrete
Prof. H. A. Haus	R. M. Bevensee	A. J. Lichtenberg
Prof. S. Saito (Visiting Fellow)	C. Fried	A. Czarapata

RESEARCH OBJECTIVES

The principal objectives of this group are:

1. Development of wideband, high-power, pulsed, klystron amplifiers.
2. Study of klystron efficiency.
3. Studies of the behavior of dense electron beams in electric and magnetic fields.
4. Study of the linear theory of coupling of modes between various propagating systems.
5. Studies of noise in electron streams.

Wideband Klystron Amplifiers. We have shown that stagger-tuned multicavity klystrons can be designed to have small-signal bandwidths of 10-15 per cent. However, little is known about the effect of this type of tuning upon efficiency. We propose to build an experimental tube of this type in order to observe its large-signal behavior. Before such a tube can be built, a number of basic building blocks will have to be developed. These are:

a. Input and output cavities with a very low Q and of specified gap impedance, $Q_L \approx 6$.

b. Cascade, bunching cavities with an adjustable, medium Q; $Q_L \approx 20$.

c. Dense, high-perveance, hollow beams; pulse power, 5-10 Mw; perveance $K = 10^{-5}$.

d. Various systems of electric and magnetic focusing.

Behavior of Dense Beams. Because of the known instability of hollow beams, further theoretical and experimental work will have to be done to determine more precisely the conditions under which such instabilities exist, and their effect upon tube performance.

Coupling of Modes. This has become a very powerful theoretical tool in the analysis of various microwave beam tubes. Further development of the basic theory and its use in solving such problems as the thick-beam traveling-wave tube, the coupling between a helix and an annular gap, and the behavior of transverse-field tubes will be undertaken.

Noise in Electron Beams. The way in which high-frequency noise is propagated on accelerated and drifting electron beams is now well understood. However, there is still doubt about the exact nature of the noise impressed upon the beam in the immediate vicinity of the virtual cathode. A number of experiments are planned that may shed some light on this problem. It is hoped that the degree of correlation between the current and velocity-noise fluctuations, and the factors affecting this correlation, may be determined.

L. D. Smullin, H. A. Haus

*This research was supported in part by Purchase Order DDL-B187 with Lincoln Laboratory, which is supported by the Department of the Army, the Department of the Navy, and the Department of the Air Force under Contract AF19(122)-458 with M.I.T.

(VI. MICROWAVE ELECTRONICS)

A. LIMITING NOISE FIGURE OF A MICROWAVE TUBE WITH A BEAM OF FINITE DIAMETER

The lower limit of the noise figure of a microwave tube with a beam propagating only two space-charge waves is known to depend only upon the input conditions beyond the potential minimum in the electron gun (1). If pure shot noise and the equivalent Rack velocity are assumed as input conditions at the potential minimum, this limit, at large gain, is

$$F_{min} = 1 + (4-\pi)^{1/2} \frac{T_c}{T} \tag{1}$$

where T_c is the cathode temperature and T is the circuit temperature. (See refs. 1, 2.)

An analysis was made to determine the lower limit of the noise figure for a finite beam diameter with input conditions at the cathode analogous to the input conditions of the one-dimensional beam that led to Eq. 1.

We assume an infinite magnetic focusing field. We further assume that the noise current from any spot of the cathode is pure shot noise and is uncorrelated with the noise from any other spot. The effect on the noise of the fields in the cathode potential minimum region is negligible. Then, for the circularly symmetric part of the excitation, the correlation function of the longitudinal, ac density J(r) at radii r_1, $r_1 + dr_1$, and r_2, $r_2 + dr_2$ of the circular cathode is

$$\overline{J(r_1)\, 2\pi r_1\, dr_1\, J^*(r_2)\, 2\pi r_2\, dr_2} = 2eI_o\Delta f \frac{2\pi r_1\, dr_1}{\pi b^2} \delta(r_1 - r_2) \tag{2}$$

where I_o is the total dc current, $\delta(r_1 - r_2)$ is the Dirac delta function, and b is the cathode radius.

Similarly, we assume that the ac velocity fluctuations at different spots of the cathode are uncorrelated and have the Rack value. It is further assumed that the single-velocity approximation is valid everywhere. In terms of the kinetic voltage V(r), the correlation function becomes (ref. 3)

$$\overline{V(r_1)\, V^*(r_2)} = \left(\frac{m}{e} u\right)^2 \frac{(4-\pi)\frac{e}{m} kT_c\Delta f}{I_o} \frac{\pi b^2}{2\pi r_1} \delta(r_1 - r_2) \tag{3}$$

where u is an average velocity at the potential minimum. Usually, the choice is

$$u^2 = \frac{2kT_c}{m} \tag{4}$$

Any excitation at the potential minimum can be expanded in terms of a complete orthogonal set of functions. The choice of the functions differs, depending upon the

practical application. (Usually, the set that is most appropriate for a subsequent WKB approximation (3) in the electron-gun region is taken.) Denote the functions of the set by $\phi_n(r)$. Normalize ϕ_n so that

$$\int_0^b \phi_n \phi_m \, 2\pi r \, dr = \delta_{nm} \tag{5}$$

when it is integrated over the beam cross section; δ_{nm} is Kronecker's delta.

We have the expansion

$$V(r) = \sum_n v_n \phi_n \tag{6}$$

$$J(r) = \sum_n i_n \phi_n \tag{7}$$

By the orthogonality condition, we obtain

$$v_n = \int_0^b V(r) \, \phi_n \, 2\pi r \, dr \tag{8}$$

$$i_n = \int_0^b J(r) \, \phi_n \, 2\pi r \, dr \tag{9}$$

Any excitation is described completely by the column matrix w, consisting of the v_n and i_n:

$$w = \begin{Bmatrix} v_1 \\ i_1 \\ \vdots \\ v_k \\ i_k \\ \vdots \end{Bmatrix} \tag{10}$$

In general, w is a column matrix of infinite order.

The kinetic power in the beam is given by

$$P_k = \mathrm{Re}\left[\int_0^b \overline{V(r)\, J^*(r)}\, 2\pi r\, dr\right]$$
$$= \sum_n \overline{v_n i_n^*} = \overline{w^\dagger Q w} \tag{11}$$

where Q is an infinite matrix with all elements zero, except for 2 × 2 matrices on its diagonal of the form

$$\frac{1}{2}\begin{pmatrix} 0 & 1 \\ 1 & 0 \end{pmatrix}$$

The dagger indicates a complex-conjugate transpose of a matrix. A noise process is determined by the correlation matrix $\overline{w w^\dagger}$. The matrix $\overline{w w^\dagger}$ contains the self-correlations and crosscorrelations,

$$\overline{v_n v_m^*}, \quad \overline{i_n i_m^*}, \quad \overline{v_n i_m^*}$$

We turn now to the evaluation of these functions. We construct

$$\overline{v_n v_m^*} = \int_0^b \int_0^b \overline{V(r_1)\, \phi_n(r_1)\, V^*(r_2)\, \phi_m(r_2)}\, 2\pi r_1\, dr_1\, 2\pi r_2\, dr_2 \tag{12}$$

Using Eq. 3, we find that

$$\overline{v_n v_m^*} = \left(\frac{m}{e} u\right)^2 \frac{(4-\pi)\left|\frac{e}{m}\right| kT_c \Delta f}{I_o} \pi b^2 \delta_{nm} \tag{13}$$

and, similarly, we find that

$$\overline{i_n i_m^*} = 2eI_o \Delta f \frac{1}{\pi b^2} \delta_{nm} \tag{14}$$

Finally, because voltage and current are assumed uncorrelated, we have

$$\overline{v_n i_m^*} = 0 \tag{15}$$

It has been shown (4) that the lower limit of the noise figure of a microwave amplifier is determined completely by the eigenvalues of the matrix

$$\overline{a\, a^\dagger}\, P$$

where a is the column vector of all normalized waves in the electron beam with the property that the kinetic power in the beam can be written as

$$P_k = \overline{a^\dagger Pa} \tag{16}$$

where P is a diagonal matrix with +1 or −1 on its (in general, infinitely long) diagonal. The column matrix a and the column matrix w used here are related by a linear transformation

$$a = Tw \tag{17}$$

Since the power is the same in both representations,

$$\overline{a^\dagger Pa} = \overline{w^\dagger T^\dagger PTw} = \overline{w^\dagger Qw}$$

we find, for an arbitrary excitation,

$$T^\dagger PT = Q \qquad \text{or} \qquad P = (T^\dagger)^{-1} Q T^{-1} \tag{18}$$

The matrix $\overline{a a^\dagger} P$ then becomes

$$\overline{a\, a^\dagger} P = T\, \overline{w\, w^\dagger}\, Q\, T^{-1} \tag{19}$$

Thus, the matrix $\overline{w w^\dagger} Q$, as obtained here, is related by a similarity transformation to the matrix $\overline{a a^\dagger} P$ of reference 4 and, therefore, must have the same eigenvalues.

According to Eqs. 12, 13, 14, and 15 and according to the nature of the Q-matrix, $\overline{w w^\dagger} Q$ is an almost diagonal matrix with all elements zero, except for 2 × 2 matrices of the general form

$$\frac{1}{2}\begin{pmatrix} 0 & \overline{|v_n|^2} \\ \overline{|i_n|^2} & 0 \end{pmatrix}$$

on its diagonal. We find that the eigenvalues λ_n of the infinite matrix $\overline{w w^\dagger} Q$ are

$$\lambda_n = \pm \frac{1}{2} \left(\overline{|v_n|^2}\ \overline{|i_n|^2}\right)^{1/2} = \pm (4-\pi)^{1/2}\, kT_c \Delta f \tag{20}$$

All eigenvalues of the $\overline{w w^\dagger} Q$ matrix are equal in magnitude. Half of the eigenvalues are positive, half are negative.

The optimum noise figure of the tube with a finite beam is given in terms of the negative eigenvalue of least amplitude. Since all negative eigenvalues are equal to $-(4-\pi)^{1/2} kT_c \Delta f$, we have (4), at large gain,

$$F_{min} = 1 + (4-\pi)^{1/2} \frac{T_c}{T} \tag{21}$$

which is the same as Eq. 1, for a one-dimensional beam.

The simplest way to obtain the optimum noise figure is the following. The gun is designed so that cross coupling among the modes is minimized. (In the WKB approximation (3) we look at the gun region as a guide of nonuniform characteristics with cross couplings among the modes that are negligible in first order.) The traveling-wave structure is designed to couple to one set of space-charge waves only. The electrode potentials in the multielectrode gun are so adjusted that they optimize the noise standing wave of this mode.

In a traveling-wave tube with a thin beam, all these conditions are approximately fulfilled. A thick beam never gives a noise figure lower than that of Eq. 21, if the noise input conditions 2 and 3 are assumed.

H. A. Haus

References

1. H. A. Haus and F. N. H. Robinson, The minimum noise figure of microwave beam amplifiers, Proc. IRE 43, 481-990 (1955).
2. W. E. Danielson and J. R. Pierce, Minimum noise figure of traveling wave tubes with uniform helices, J. Appl. Phys. 25, 1163-1165 (1954).
3. H. E. Rowe, Shot noise in electron beams at microwave frequencies, Sc.D. Thesis, Department of Electrical Engineering, M.I.T., Oct. 1952.
4. F. N. H. Robinson and H. A. Haus, Analysis of noise in electron beams, J. Electronics 4, 373-384 (Jan. 1956).

B. CAVITY-TO-HELIX COUPLING

A microwave tube for use in klystron research will be built. In this tube the beam is enclosed by a glass envelope in such a way that klystron cavities can be placed external to the vacuum envelope. In order to prevent electrostatic charging of the glass, a helix will be inserted between the beam and the glass tube. It will have a phase velocity that is much less than the beam velocity. For this device to operate as a klystron, the helix must introduce no direct coupling between the cavities.

For the determination of the gap length that will give minimum coupling between cavity and helix we can make a static expansion of the gap fields in terms of the

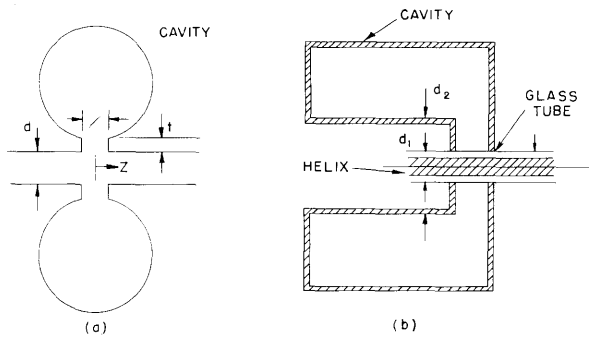

Fig. VI-1. Cavity-helix coupling system.

Fourier integral and assume that this minimum occurs when the coefficient of the term corresponding to the helix propagation constant, β, becomes zero. This coefficient can be evaluated by considering the field at the gap edge. If t/d in Fig. VI-1a is large, we might assume a constant field across the gap at r = d/2, as is commonly done in the evaluation of klystron beam coupling. In this case, the coefficient contains the factor

$$\frac{\sin \beta\ell/2}{\beta\ell/2}$$

which would indicate minimum coupling at $\beta d = 2\pi$ radians. If t/d is small and ℓ tends to zero, the voltage at the edge is given by

$$V = \frac{1}{\pi} \sin^{-1} \frac{2z}{d}$$

which gives a coefficient that contains $J_o(\beta d/2)$, thus indicating minimum coupling at $\beta d = 4.81$ radians. Experimental evaluation of the cavity at 1200 mc, as shown in Fig. VI-1b, in which $d_2/d_1 = 3.3$, indicates a sharp minimum at a value of $\beta\ell$ lying between these two extreme values.

B. A. Highstrete

C. HOLLOW-BEAM FOCUSING

The problems associated with the realization of Harris flow (1) have been described by Harris (2) and by Crumly (3). The problems are primarily associated with the magnetic leakage field around the cathode.

Cook (4) described a method of producing a modified Harris flow. A pair of opposing coils excites the iron circuit in such a way that a flux pattern is produced, as shown in Fig. VI-2. The gun is placed in the fringing field of the annular gap; therefore $B_z = 0$ at the middle of the beam. The radial field falls off nearly exponentially,

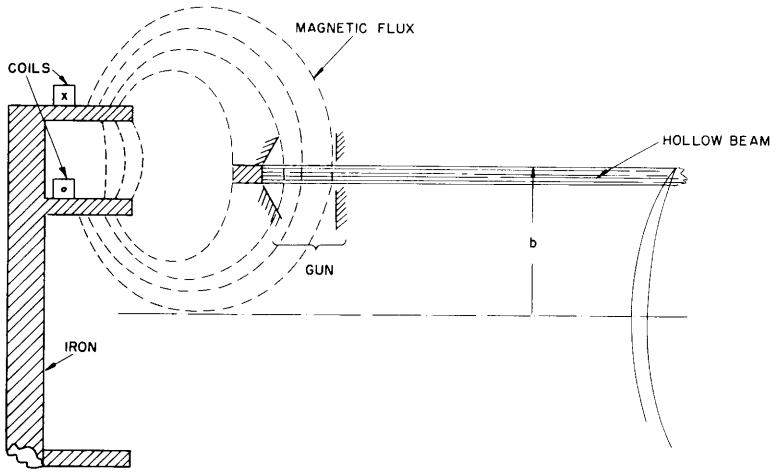

Fig. VI-2. Cook's modification of Harris-flow focusing.

so that $B_r \approx B_o e^{-pz}$. With this arrangement, the requirement that no flux is normal to the cathode surface can be nearly satisfied, and the field at the anode can be made a small fraction of the field at the cathode.

Although Cook described a focusing system that was built around these ideas, no detailed analysis of the beam behavior exists. We have a beam accelerated under space-charge-limited conditions in the presence of a transverse magnetic field. If it is assumed that the magnetic field is purely radial in the neighborhood of the beam and behaves as

$$B_r = B_o \frac{e^{-pz}}{r}$$
$$B_z = 0 \tag{1}$$

then the equations of motion are

$$\ddot{r} = \eta E_r + \frac{a^2}{r^3 p^2} (1 - e^{-pz})^2 \tag{2}$$

$$\ddot{z} = \eta E_z - \frac{a^2}{r^2 p} (1 - e^{-pz})\, e^{-pz} \tag{3}$$

where $a = \eta^2 B_o^2 r_o^2$.

In Eq. 2 we see an added centrifugal acceleration because of the rotation of the beam. The electric fields E_r and E_z are the resultants of space-charge and electrode potentials.

The problem is to find a set of electrode shapes that will make $\ddot{r} = 0$, when the

current I_o, voltage V_o, and total flux $\phi = \int_0^d B_r \, dz$ are specified. The present plan is to instrument the analog computer of the Dynamic Analysis and Control Laboratory, M.I.T., to plot the trajectories corresponding to Eqs. 2 and 3 with the aid of an electrolytic tank. The procedure will be as follows:

1. Design a hollow-beam Pierce gun of the desired perveance and size.
2. Set up the resultant electrode system in an electrolytic tank, with space charge simulated by injected current.
3. Use the analog computer to plot the trajectory of an edge electron, with fields picked up from the tank.
4. Correct the electrode system until the trajectory indicates $\ddot{r} \approx 0$.

L. D. Smullin, P. G. Pantazelos, G. H. Pfersch, Jr.

[Mr. Pantazelos and Mr. Pfersch are members of the Dynamic Analysis Control Laboratory.]

References

1. L. A. Harris, Axially symmetric electron beam and magnetic-field systems, Technical Report 170, Research Laboratory of Electronics, M.I.T., June 1952.
2. L. A. Harris, Hollow beams in electrostatic fields, Technical Note HB-2N, University of Minnesota, May 1955.
3. C. B. Crumly, Theory and application of uniform electrostatic focusing of hollow beams, Technical Report 457-1, Stanford University, Nov. 1, 1955.
4. Described at IRE Conference on Electron Tube Research, Boulder, Colorado, 1956.

D. HOLLOW-BEAM GUN DESIGN

With the use of the electrolytic tank, two hollow-beam guns of perveance $K = 10^{-5}$ were designed. They are of parallel-flow design with beam thickness $t = b/10, b/5$ (b being the outer beam radius). A mechanical design of the $t = b/10$ beam gun is being prepared.

Following the work of L. A. Harris (1), we are making a study of convergent (toroidal) hollow-beam guns.

A. Czarapata, C. Fried

References

1. L. A. Harris, Research on hollow dense electron beams, Technical Report HB-2R, University of Minnesota, Sept. 1955.

E. LOW-Q CAVITY DESIGN

In a high-power klystron ($P_o \approx 5$ Mw) with a beam of perveance $K = 10^{-5}$, a cavity that is loaded so that it almost stops a tightly bunched beam will have a loaded Q, $Q_L \approx 6$, with a gap impedance, $R \approx 400$ ohms. In order to produce a minimum-Q cavity, it is important that there be little or no stored energy in addition to that unavoidably stored in the gap capacitance. (The latter is fixed by electronic considerations.) A further requirement is that the electric field at the gap have a high degree of angular symmetry.

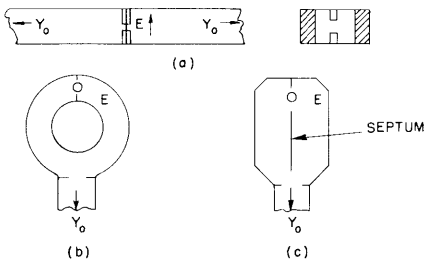

Fig. VI-3. Evolution of low-Q cavity.

A coplanar resonator, loaded from two sides, appears to be an excellent scheme for achieving these requirements. Successive developments of this idea are shown in Fig. VI-3.

The final development in Fig. VI-3c would be made by:

1. making a wideband, matched, 180° bend, without the resonant structure in place;
2. making a wideband junction between the output guide and the two parallel guides;
3. adjusting the gap and the inductive iris to resonate at the desired frequency.

L. D. Smullin

F. MULTICAVITY KLYSTRONS*

In the Quarterly Progress Report of October 15, 1956, page 34, we presented the small-signal theory of multicavity klystron operation. With the help of this theoretical formulation, we shall now analyze the gain-phase characteristics of these tubes. The problem of importance is the broadbanding of multicavity klystrons. This can be achieved through stagger tuning of the cavities and proper separation between cavities. Thus the interrelations between gain, bandwidth, length of the tube, and number of cavities in the tube will be studied.

1. Theory of Stagger Tuning

The gain of a multicavity klystron was shown to be proportional to

$$\left| Z_{in}\, Z_{out}\, \frac{I}{V} \right|^2 \qquad (1)$$

*This work was sponsored in part by the Office of Naval Research under Contract Nonr 1841(05).

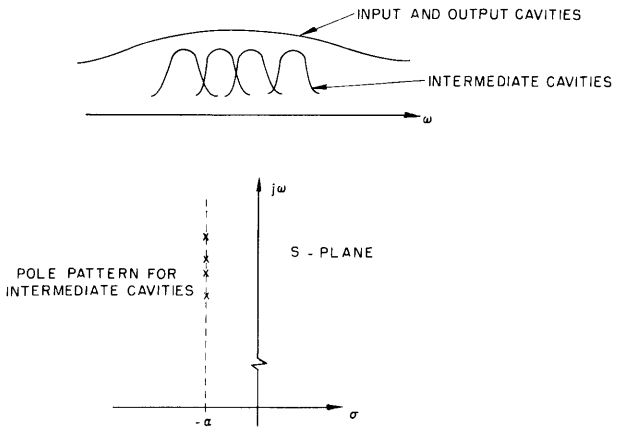

Fig. VI-4. Multicavity klystron stagger tuning; equal-Q intermediate cavities.

where Z_{in} and Z_{out} are the input and output cavity-gap impedances, and I/V is a characteristic of the intermediate cavities. Figure VI-4 shows, in general terms, the method of stagger tuning that was chosen. The input and output cavities are low-Q, and cover the band which is of interest. The intermediate cavities are stagger-tuned on an (approximate) equal-Q line in the complex frequency plane. Since the input and output cavity characteristics enter into Eq. 1 in a multiplicative way, only the intermediate-cavity gain characteristic I/V has to be evaluated.

It is now convenient to introduce some normalizations and appropriate approximations into the expression for I/V. We shall illustrate this for a four-cavity klystron that has equidistant spacing between cavities. In general,

$$\frac{I}{V} = -j\, Y_o^3 \sin^3\theta \quad z_1 z_2 + Y_o^2 \sin\theta \sin 2\theta \quad (z_1 + z_2) + j\, Y_o \sin 3\theta \tag{2}$$

where θ is the plasma transit angle between cavities, Y_o is the characteristic admittance of the drift, and $z_i = M^2 Z_i$. Thus

$$Z_i = \frac{1}{C} \frac{s}{(s - s_i)(s - s_i^*)} \tag{3}$$

where C is the gap capacitance, $s = \sigma + j\omega$ is the complex frequency variable, and $s_i = -\alpha + j\omega_{di}$ gives the pole position for the i^{th} cavity.

For the band of frequencies between half-power gain points, a good approximation to Eq. 3 is

$$Z_i \approx R \frac{1}{1 + jx_i} \equiv R\, F_i(x) \tag{4}$$

where $x_i = 2Q \frac{\omega - \omega_{oi}}{\omega_{oi}} = \frac{\omega - \omega_{oi}}{a}$, and $R = \frac{1}{G}$ is the total gap resistance. We now introduce a gain-per-stage quantity,

$$g = \frac{M^2 Y_o}{G} \sin\theta \tag{5}$$

and a normalized intermediate-cavity gain,

$$K = \frac{I}{V} \frac{1}{Y_o \sin\theta} \tag{6}$$

Substitution of Eqs. 4 and 6 in Eq. 2 gives

$$K = -j\, g^2 F_1 F_2 + g \frac{\sin 2\theta}{\sin\theta} (F_1 + F_2) + j \frac{\sin 3\theta}{\sin\theta} \tag{7}$$

The choice of tube fixes θ and g; and F_i is the frequency-dependent quantity.

2. Analog Computer Results

In general, the complexity of the gain expression does not allow a simple evaluation of multicavity-klystron bandpass characteristics. The analog computer of the Dynamic Analysis and Control Laboratory, M.I.T., was used for this purpose. The range of the tube designs that have been investigated is shown in Table.VI-1.

Table VI-1. Multicavity Klystron Tubes Investigated.

Four-cavity klystron: $\frac{M^2 Y_o}{G} = 29.4$; $Q_L = 110$

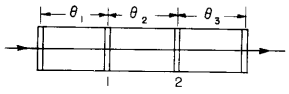

	θ_1	θ_2	θ_3	
1.	20°	20°	20°	
2.	53.2	53.2	53.2	(VA-87)
3.	90	90	90	
4.	35	35	90	
5.	70	20	70	
6.	90	90	20	
7.	90	90	60	
8.	20	90	90	
9.	60	90	90	
10.	90	20	90	
11.	90	60	90	

Seven-cavity klystron: $\frac{M^2 Y_o}{G} = 29.4$; $Q_L = 110$

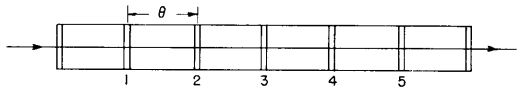

	θ
1.	26.6°
2.	45
3.	90

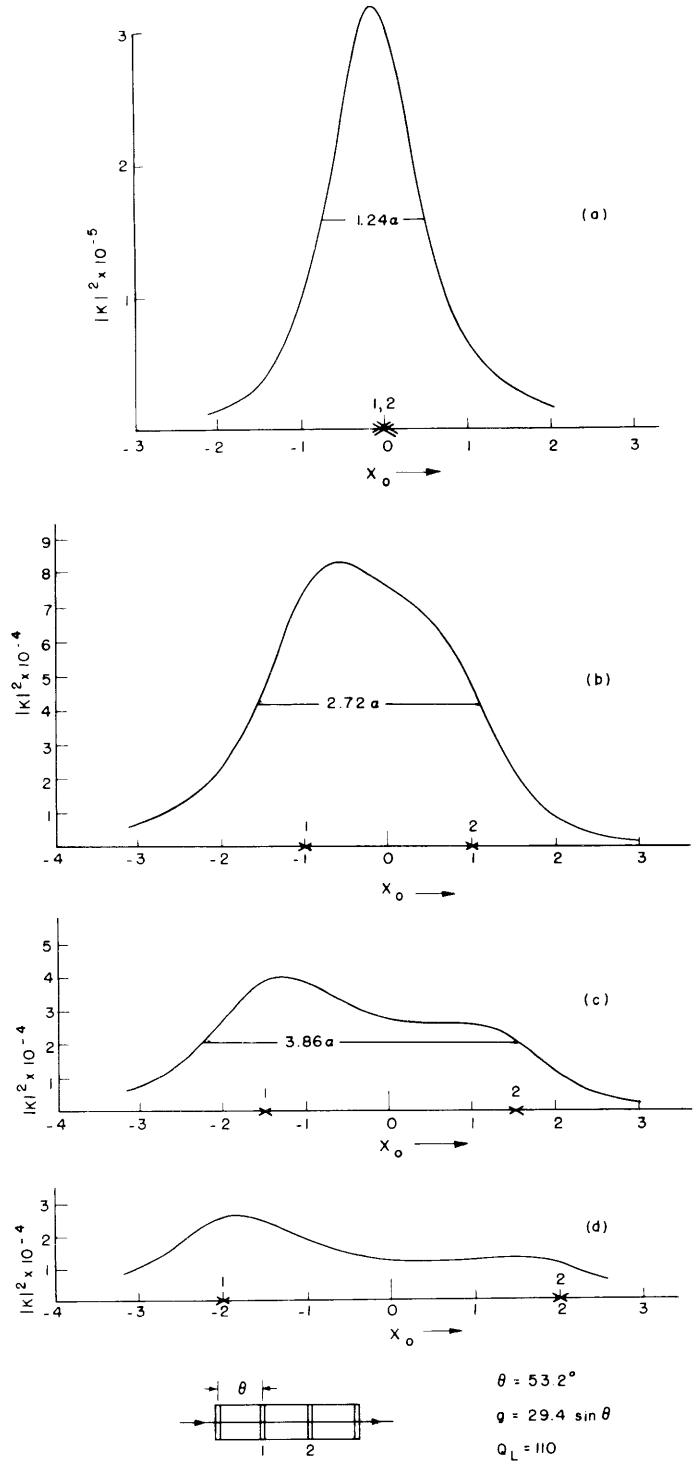

Fig. VI-5. Gain versus frequency for a four-cavity klystron (corresponding to VA-87); successive cavities spaced equidistantly; detuning between cavities varied.

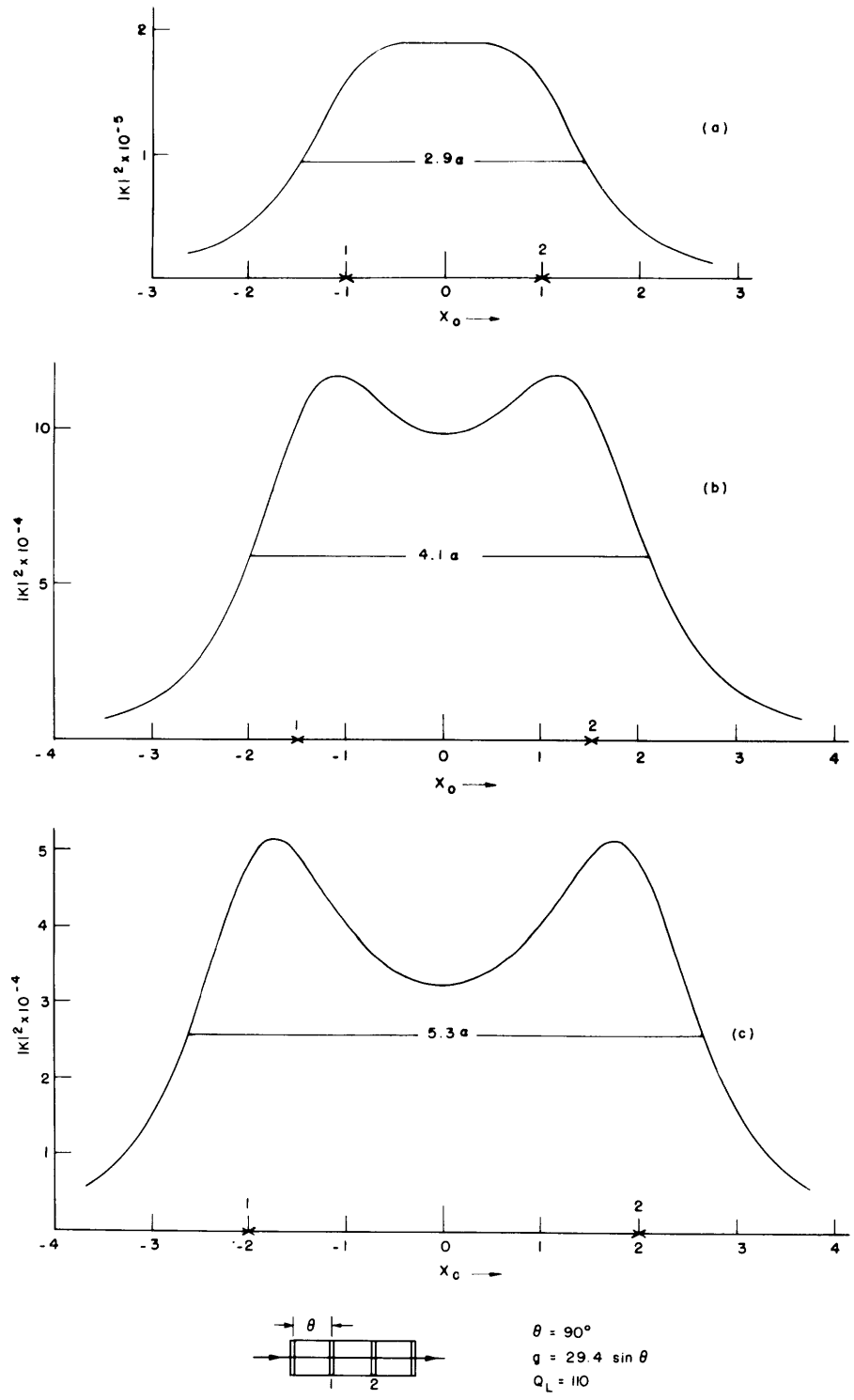

Fig. VI-6. Gain versus frequency for a four-cavity klystron; successive cavities spaced equidistantly; detuning between cavities varied.

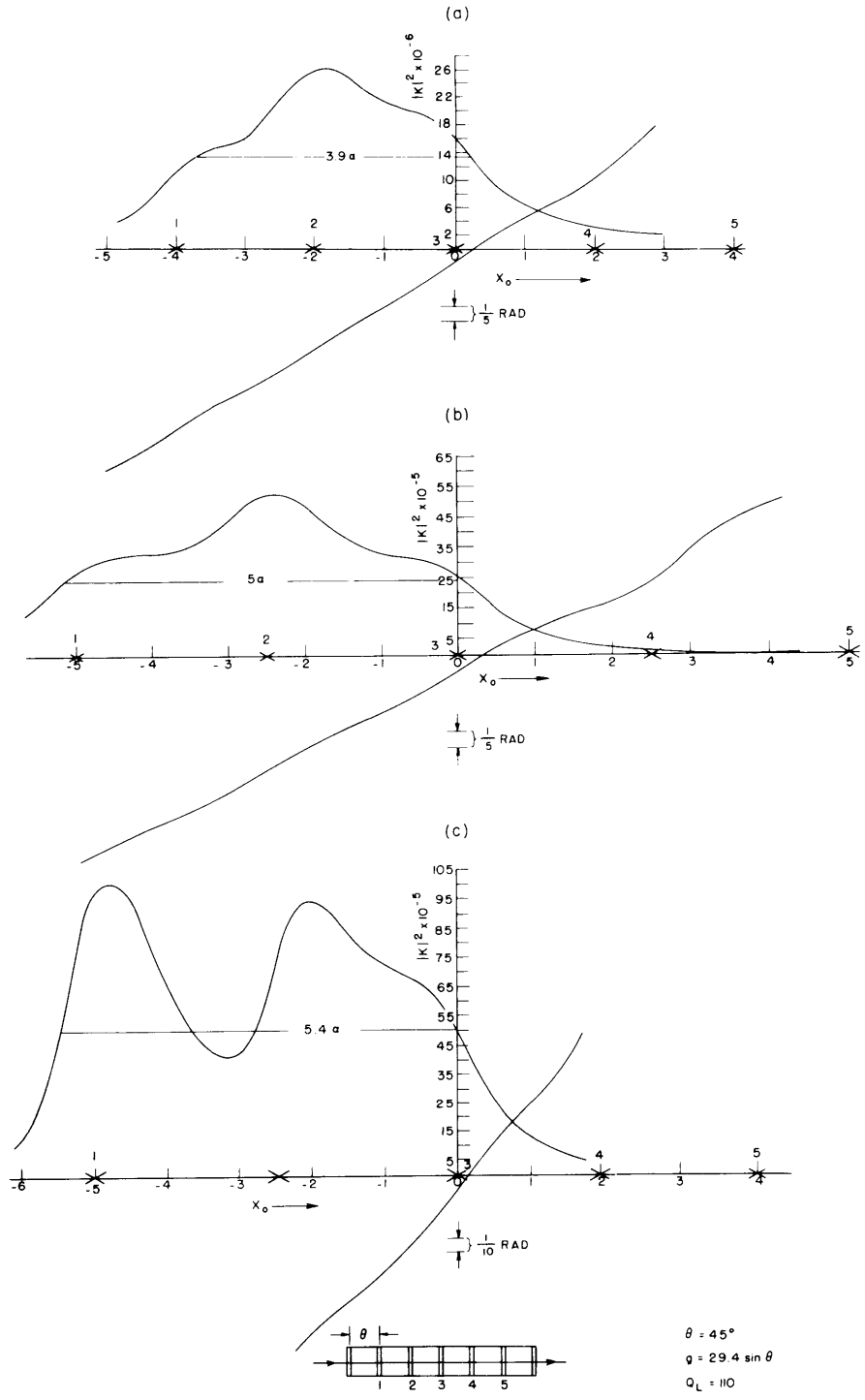

Fig. VI-7. Gain and phase versus frequency for a seven-cavity klystron; successive cavities spaced equidistantly; detuning between cavities varied.

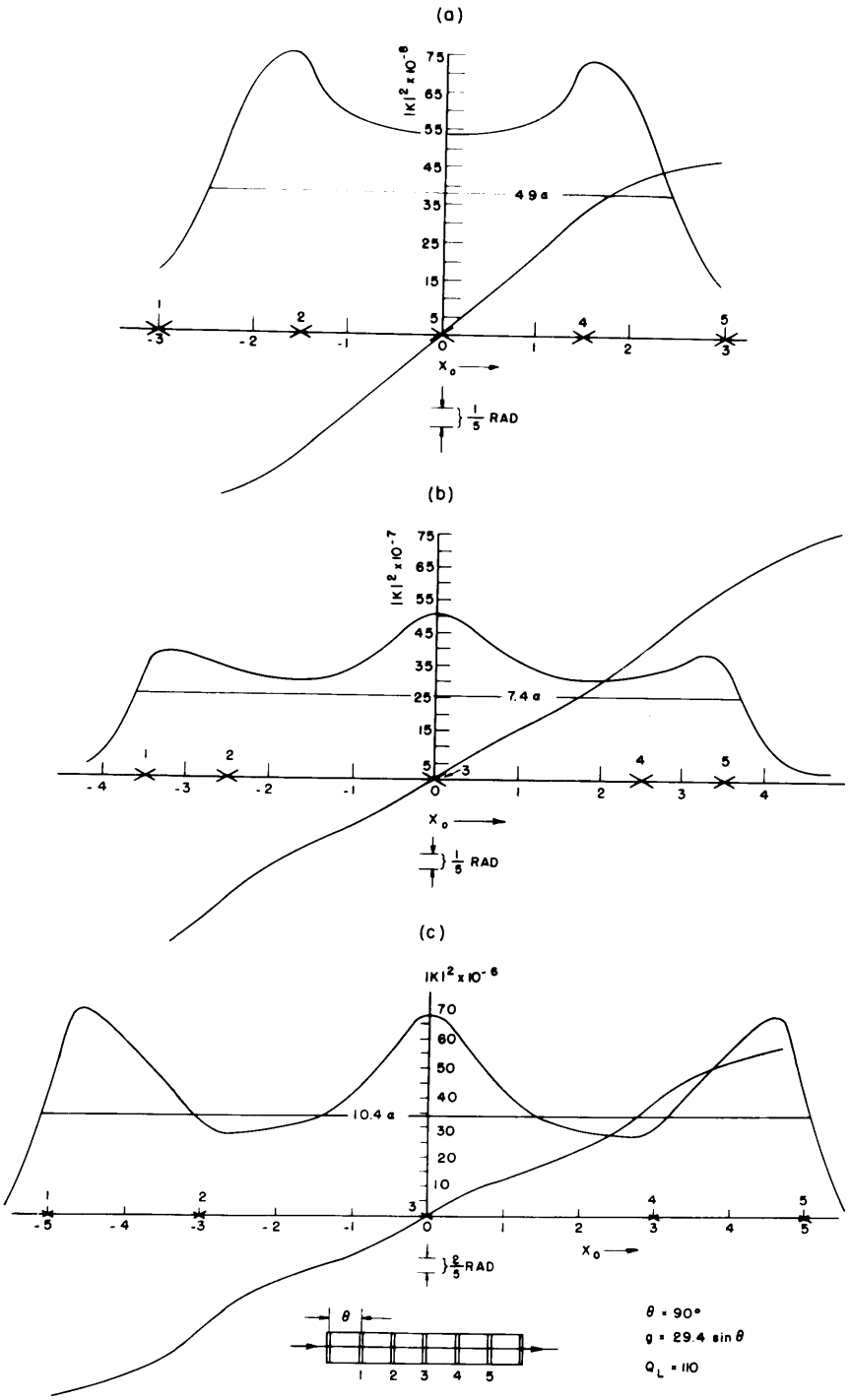

Fig. VI-8. Gain and phase versus frequency for a seven-cavity klystron; successive cavities spaced equidistantly; detuning between cavities varied.

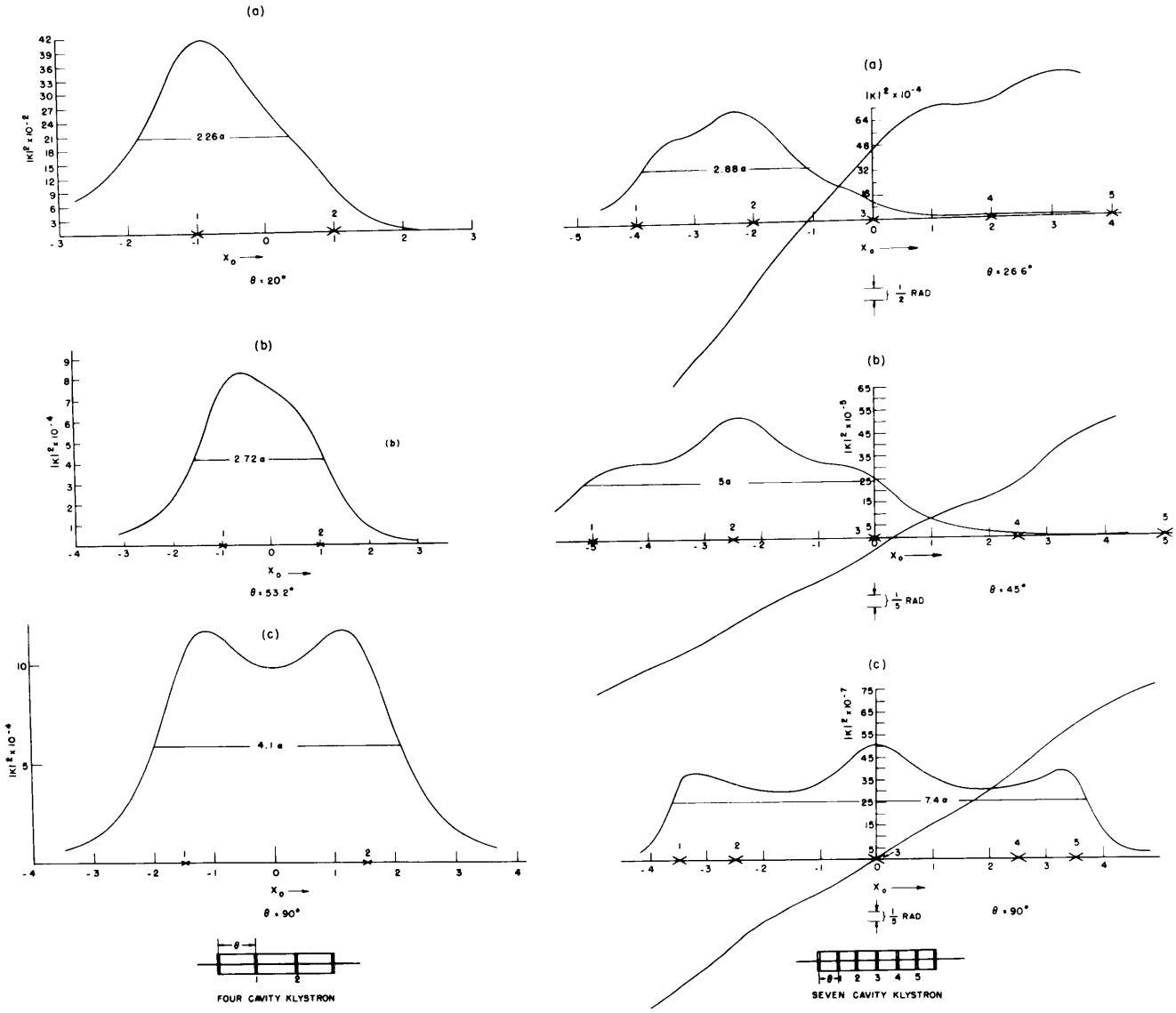

Fig. VI-9. Gain bandwidth variation as a function of tube length for a four- and a seven-cavity klystron. Spacing between successive cavities is the same, and equal to θ.

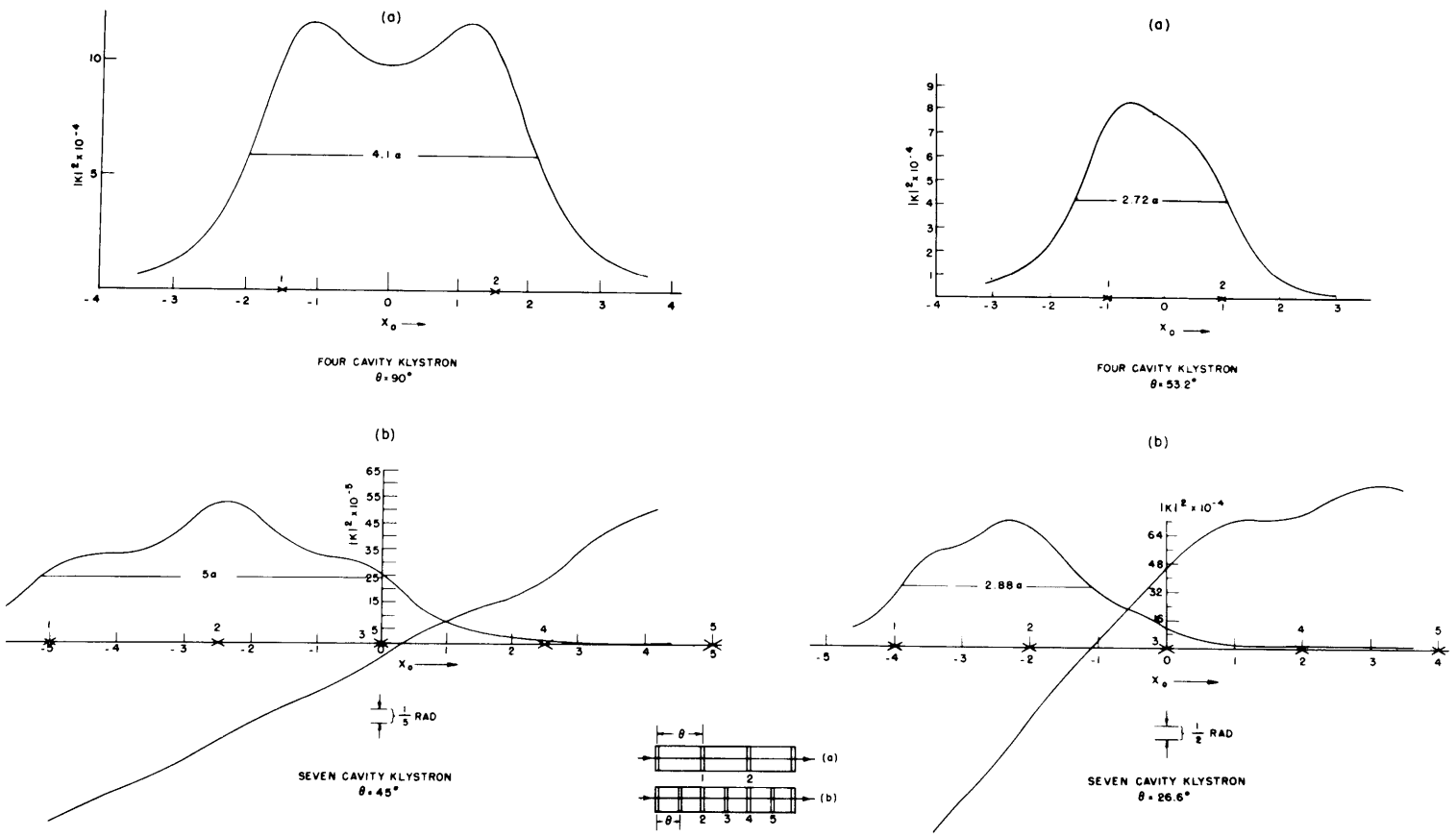

Fig. VI-10. Gain-bandwidth variation as a function of the number of cavities in a fixed length of tube. In each case successive cavities are spaced θ° equidistantly.

Results for the six-cavity klystron have already been presented (1). The results for the four- and seven-cavity tubes will now be summarized. The gain-per-stage parameter g for these results corresponds to the Varian Associates VA-87 high-power four-cavity klystron (2) on which measurements were previously made.

Figures VI-5, VI-6, VI-7, and VI-8 show typical results obtained on the computer. The intermediate-cavity power gain $|K|^2 = \left| \frac{I}{V} \frac{1}{Y_o \sin\theta} \right|^2$ is plotted versus the normalized frequency parameter $x_o = \frac{\omega - \omega_o}{\alpha}$, where ω_o is a chosen angular frequency in the band of interest. (For the tubes investigated, $\omega_o/2\pi = 3000$ mc was used.) The resonant frequency of each cavity is indicated by a cross mark on the x_o axis. The tube bandwidth (between half-power points) is indicated in terms of α, the half-bandwidth of a single intermediate cavity. For the $\theta = 90°$ klystrons the order of the cavities in the tube was selected to give a symmetrical, optimum, gain-bandwidth response. This optimization follows directly from a careful inspection of the feedforward terms.

Figures VI-9 and VI-10 indicate the interrelations between the gain bandwidth, length, and complexity of the tube which were sought.

Only a selected number of curves are shown to illustrate our conclusions. Figure VI-9 shows the gain-bandwidth variation in a tube with a fixed number of cavities when the length of the tube is varied by increasing the separation between successive cavities. In both the four- and seven-cavity klystrons, the gain bandwidth increases as the separation between the cavities increases and is maximum when $\theta = \pi/2$ (i.e., $\lambda_q/4$ separation). Figure VI-10 shows the gain-bandwidth variation in a tube of fixed length when the number of cavities is varied. Here, again, the gain-bandwidth product increases, but the increase becomes less as the separation between cavities is reduced. Other cross sections through the data indicate that the same conclusions follow.

The observed behavior can be explained in terms of the physical gain mechanism which the feedforward terms express mathematically.

ERRATA: Quarterly Progress Report, October 15, 1956, page 35.

1. In captions for Figs. V-6 and V-8: For "impedance," read "admittance."
2. Fig. V-9: In equation for I/V, the fourth line, read

$$-j\, Y_o^3 \sin^2 2\theta \sin\theta \,(z_1 z_3 + z_2 z_4 + z_2 z_3)$$

A. Bers

References

1. A. Bers, IRE-AIEE 14th Annual Conference on Electron Tube Research, June 27-29, 1956.
2. B. A. Highstrete, Quarterly Progress Report, Research Laboratory of Electronics, M.I.T., Oct. 15, 1956, pp. 37-38.